IOP Conf. Series: Journal of Physics: Conf. Series **830** (2017) 012072 doi:10.1088/1742-6596/830/1/012072

Multiscale models of metal behaviour and structural change under the action of high-current electron irradiation

A E Mayer, V S Krasnikov, P N Mayer, V V Pogorelko

Department of Physics, Chelyabinsk State University, Bratiev Kashirinykh Street 129, Chelyabinsk 454001, Russia

E-mail: mayer@csu.ru

Abstract. We present our models of the tensile fracture of metals in the solid and molten states, the melting and the plastic deformation of the solid metals. Also we discuss implementation of these models for simulation of the high current electron beam impact on metals. The models are constructed in the following way: the atomistic simulations are used at the first stage for investigation of dynamics and kinetics of structural defects in material (voids, dislocations, melting cites); equations describing evolution of such defects are constructed, verified, and their parameters are identified by means of comparison with the atomistic simulation result; finally, the defects evolution equations are incorporated into the continuum model of the substance behaviour on the macroscopic scale. The obtained continuum models with accounting of defects subsystems are tested in comparison with the experimental results known from literature. The proposed models not only allow one to describe the metal behaviour under the conditions of intensive electron irradiation, but they also allow one to determine the structural changes in the irradiated material.

1. Introduction

Impact of the high-current electron beam [1-4] on a metal provokes a variety of non-equilibrium dynamic processes. The main effect of the beam is in the rapid heating of substance inside the energy absorption area accompanied by melting. The range of the fast electron reaches half a millimetre or more for the electron energy of about 1 MeV [1-3]. Using the value of 5 km/s as a typical sound velocity in solid metals, one gets the mechanical relaxation time [4] of about 100 ns. Therefore, an electron irradiation pulse with the duration of about several tens of picoseconds produces heating in an almost isochoric mode similar to the powerful femtosecond laser pulses [5,6]. The isochoric heating increases pressure up to several tens of gigapascals [1-3] at the typical beam parameters. The subsequent expansion of the heated and stressed surface layer produces a compression pulse consisting of a shock wave followed by a rarefaction wave and propagating deep into the irradiated metal. The compression pulse induces the dynamic plastic deformation with a substantial change of the material microstructure [3], and the pulse reflection from the rear free surface of the irradiated sample can lead to the tensile (spall) fracture [1-3,7]. The melt inside the energy absorption area also reveals a rich physical behaviour. The melt expends initially due to the pressure gradient, and then by inertia. The expansion by inertia transfers the melt into the metastable state at a negative pressure, which leads to the tensile fracture of melt by means of cavitations [8,9]. A complete mathematical model of the high current electron beam interaction with metals should take into account all the mentioned processes. Among other things, this model is required for interpretation of the electron beam experiments [1-3].

2. Mathematical model

We use the multiscale approach for construction of the mathematical model. Atomistic simulations are used for the investigation of the elementary processes in the defect subsystems, such as growth of voids or melting sites, motion of dislocations etc. It allows us to define the form and parameters of the kinetic equation for defect ensembles. The obtained regularities are generalized on the continuum level, which is applicable for modeling of the dynamics of the macroscopic volumes of metal under irradiation. Continuum model supposes an averaged description of the lattice defects in the form of various parameter fields (scalar density of dislocations, concentration and size of voids or melting sites). For description of the non-equilibrium melting, it is supposed that each substance element consists of a mixture of the solid and molten parts.

The continuum model consists of a standard set of the continuum mechanics equations supplemented by models for specific physical processes and properties. The wide-range equations of state [10,11] are used for calculation of the pressure and temperature as functions of density and internal energy. The electron beam action is described by means of the energy release function D, which is calculated from the solution of the fast electron transport problem using the method [12]. The molecular dynamic (MD) simulations are performed with the help of LAMMPS [13] and various interatomic potentials based on the embedded atom model. These simulations are used for construction and verification of the plasticity, fracture and melting models [8,14-18]. The fracture model [8,16-18] describes the nucleation, growth and coalescence of voids including the late stage with the predomination of the voids interaction [9]. The plasticity model [14,19,20] describes the plastic deformation tensor increment as a result of the dislocation motion with velocity determined by the acting stresses; the dislocation kinetics takes into account generation, annihilation and immobilisation of dislocations. The continuum model of melting [21] is based on the description of the current phase state by means of fields of concentration and size of the melting sites; the site size is supposed to be much less than the typical spatial scale of the considered problem; so, the interfaces are not traced explicitly, but an averaged picture is considered instead. Two model problem statements are used in MD simulations of melting for determination of the model equations and coefficients: (i) reaching of the equilibrium in an isolated system with a flat interface between solid and liquid; (ii) melting of an initially homogeneous monocrystal heated by a source with a constant power.

Verification of the model had been performed by means of comparison of the modelling results both with the MD simulations and the experimental data known from literature. For verification of the plasticity and fracture models, we compare the modelling results with the high-velocity impact experiments, which are the standard test of the dynamic properties of various materials.

3. Application for the high-current electron irradiation problem

The continuum model is applied to the calculation of the stainless steel dynamics under the action of the high-current electron beam of the SINUS-7 accelerator (Tomsk, Russia, Institute of High Current Electronics SB RAS) [1-3]. The beam parameters are the following: the maximal energy of fast electrons is 1.35 MeV, the pulse duration is 45 ns (full-width on half-maximum), the maximal power density in the center of the beam is 34 GW/cm^2, and the incident energy density is 1.2 kJ/cm^2; the experimentally determined oscillograms of the beam current and the accelerating voltage are used [3].

Figure 1 shows the spatial distributions of the stress tensor components in the consequent moments of time. The electron beam acts on the left side of the sample and induces an intensive heating up to 8000 K, and the following melting and ablation of matter inside the energy absorption area (the fast expanding part of the sample). The thickness of the energy absorption area is about 1 mm; therefore, the heating is close to an isochoric one. Compressive stress reaches 33 GPa at 50 ns from the irradiation beginning [3]. The expansion of the heated material becomes substantial starting at approximately 50-100 ns from the beginning of the irradiation; the compressive stresses rapidly decrease thereafter. The running shock wave is formed with the initial amplitude of 17 GPa and with a duration of the compression pulse of 0.2 μs. The duration of the compression pulse is restricted by the unloading wave, which propagates from the free surface behind the shock wave. An additional

unloading wave originates from the side unloading and converges to the target axis. Interference of two unloading waves creates an expansion wave with tensile stresses following the shock wave; the values of tensile stresses grow up as this unloading wave converges to the sample axis. The expansion wave reaches the target axis at the moment when the shock wave passes the distance of about the beam radius. The shock wave amplitude decreases with propagation deep into the target and the duration of the compression pulse increases due to the interactions with the following expansion wave. An elastic precursor with the amplitude of 1 GPa propagated at the head of the shock wave.

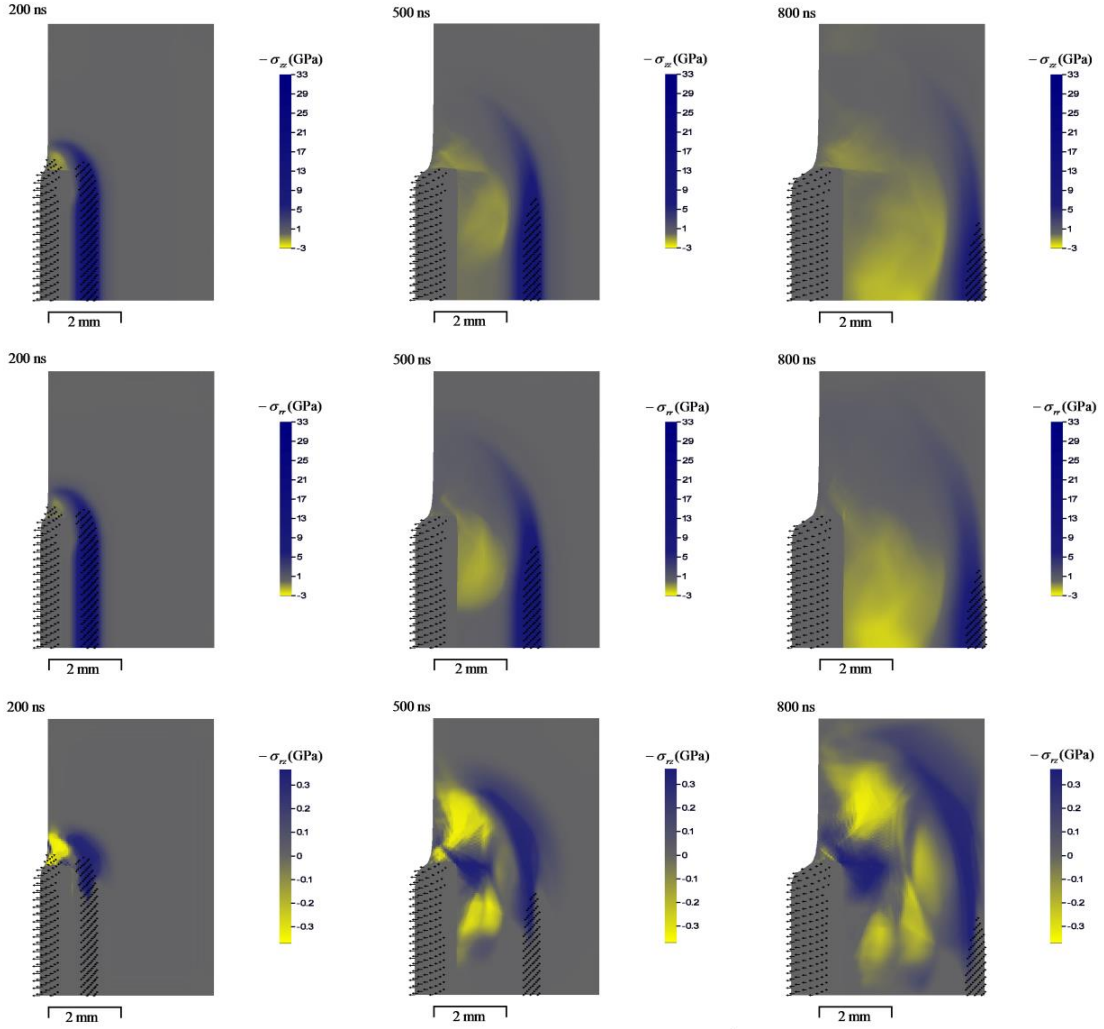

Figure 1. Calculated distributions [3] of the stress tensor components in stainless steel sample with the thickness of 4.5 mm in consequent moments of time (200, 500 and 800 ns) after beginning of the irradiation; stresses are shown with negative sign. Electron beam (SINUS-7 accelerator) irradiates the left side of the target; axial direction is horizontal one and radial direction is vertical one. Little arrows show the substance velocity vectors.

Calculated spatial distributions of the volume fracture of voids for the various sample thicknesses are presented in figure 2. One can see a distinct fracture area near the rear surface that is formed at the shock wave reflection. For the targets thinner than 6.5 mm, the condition of complete fracture is realized within this area, while only an incomplete fracture takes place for the thicker samples. Although, for thicknesses 9 mm, the maximal tensile stress along the sample axis exceeds the spall strength, the decrease of the acting stresses with radius prevents the complete fracture. The expected positions of the main cracks or the incomplete fracture zones are schematically shown in figure 3,

which are determined as widest in radial direction cross-sections within the fracture area. The distances between such cross-section and rear surface are the calculated thicknesses of the spalled layer, which are plotted in figure 6 along with the experimental results taken from [3]. Both experimental and calculated dependences are close to linear functions and correlate with each other.

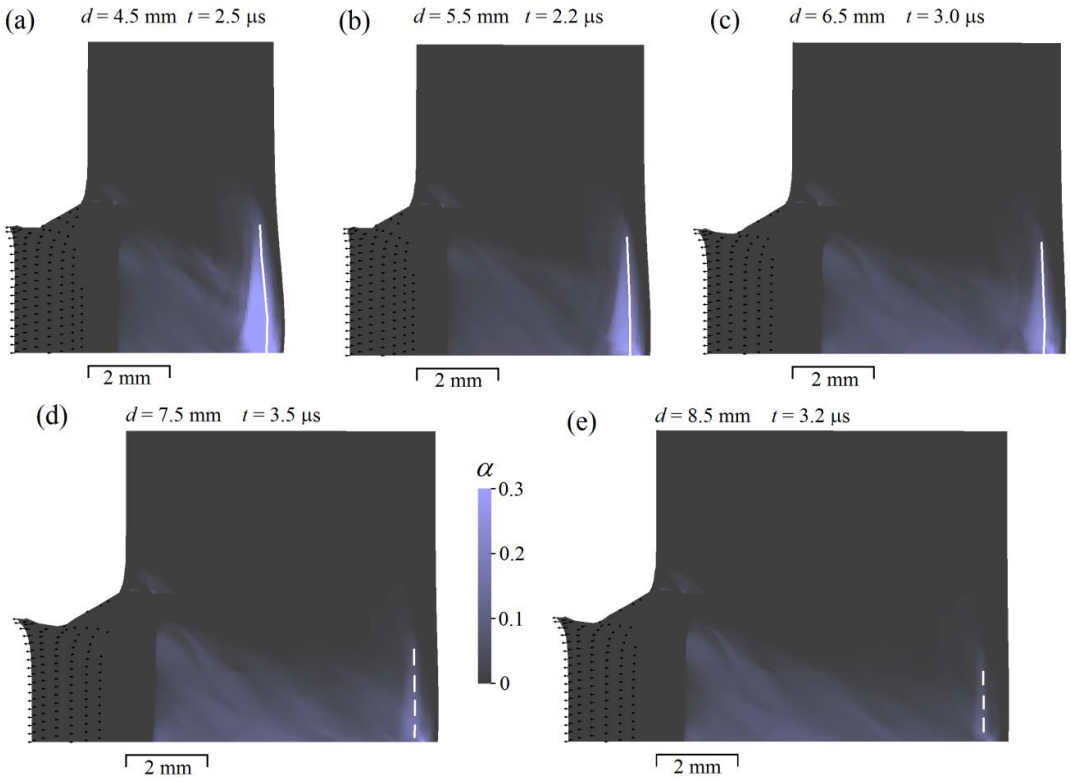

Figure 2. Calculated distributions of the volume fraction of voids α in samples with various thicknesses made of stainless steel and irradiated by the high-current electron beam (SINUS-7 accelerator [1-3]). (a,b,c) solid lines show the expected position of the main crack, (d,e) dashed lines show the expected position of the zone of incomplete fracture. Expanding cloud of ablated material is from the left. Little arrows on the left sides show the substance velocity vectors for the expanding ablated matter.

Influence of the non-equilibrium melting [21] on the temperature distribution in the irradiated aluminum is shown in figure 4, which presents the spatial distributions of the substance temperature T, the melting temperature T_m depending on the local pressure and the volume fraction $(1-\alpha_m)$ of solid phase for time moments 25 and 30 from the beginning of irradiation.

The considered electron beam heats the aluminum layer 2 mm in thickness; spatial distribution of the energy release power is non-uniform which leads to the non-uniform temperature distributions. The energy release power reaches 0.08 PW/kg in maximum which leads to the heating rate of about 70 K/ns. Complete melting occurs in the central part of the energy absorption area to the moment of time of 25 ns. Temperature of the uniform melt begins to exceed T_m in this central area, while it is close to T_m at the edges of the complete melting zone. Two regions of partial melting adjoin the complete melting zone from both sides. $T \approx T_m$ in the internal parts of these partial melting regions which implies reaching the phase equilibrium; increase in the melt volume fraction goes here to the extent of energy supply by the beam. Aluminum is overheated $T > T_m$ within the external parts of the partial melting zones; the melt volume fraction goes here at the expanse of both the energy transfer

from by beam and the leaving the metastable overheated state. Areas of overheated solid metal adjoin the partial melting zones. The overheating reaches $T - T_m \approx 100\ K$. The left zone of partial melting disappears at the time moment of 30 ns; aluminum becomes completely melted up to the exposed free surface. The right zone of partial melting moves deep into the target in the course of time; the molten layer thickness increases till the beam action termination.

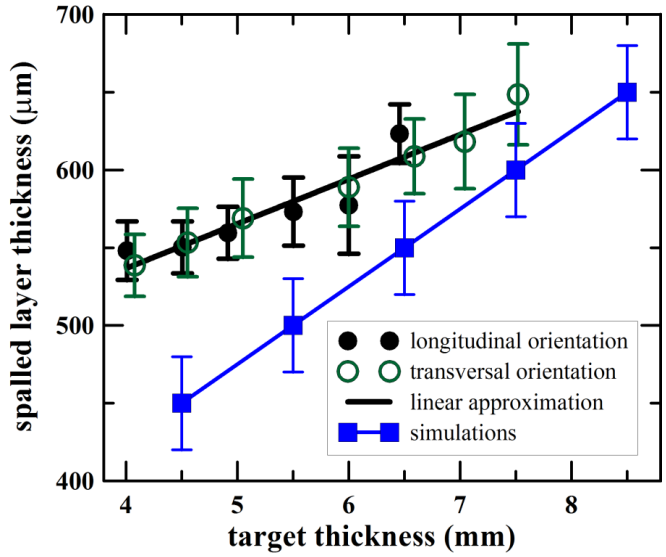

Figure 3. Experimental [3] and calculated dependencies of the spalled layer thickness on the sample thickness for stainless steel. Experimental points correspond to both the longitudinal and the transversal orientations of the δ-ferrite interlayers relative to the shock wave propagation direction [3].

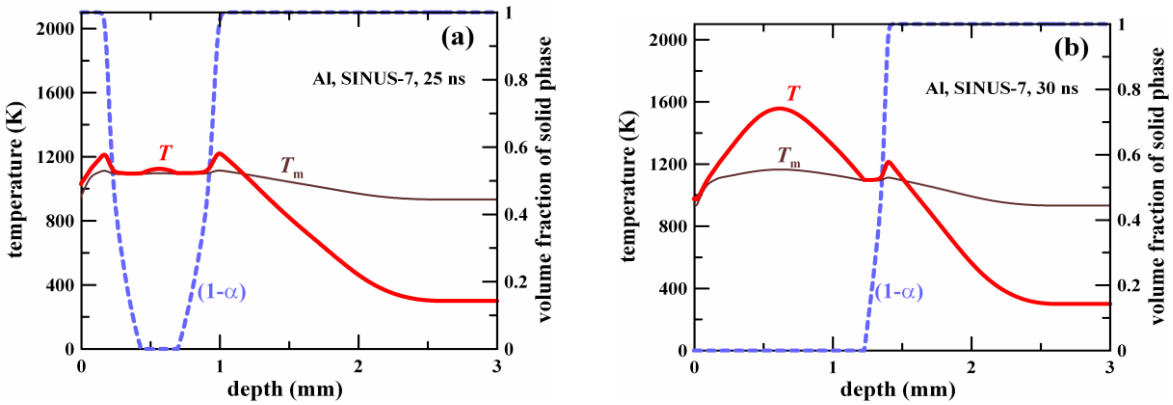

Figure 4. Spatial distributions of the substance temperature T (thick solid lines), the melting temperature T_{m} (thin solid lines) and the volume fraction $(1-\alpha_m)$ of solid phase (dash lines) in the consequent moments of time: irradiation of aluminum by the high-current electron beam with parameters of SINUS-7 accelerator. Initial target thickness is 3 mm; the electrons of the beam fall normally on the left surface of target.

4. Conclusion

Here we present our models of the tensile fracture of metals in the solid and molten states, the melting and the plastic deformation of the solid metals. Also we discuss implementation of these models for simulation of the high current electron beam action on metals. The models are constructed in the following way: the atomistic simulations are used at the first stage for investigation of dynamics and kinetics of structural defects in material (voids, dislocations, melting cites); equations describing the evolution of such defects are constructed, verified, and their parameters are identified by means of comparison with the atomistic simulation result; finally, the defects evolution equations are incorporated into the continuum model of the substance behaviour on the macroscopic scale. The

obtained continuum models with accounting of defects subsystems are tested in comparison with the experimental results known from literature. The proposed models not only allow one to describe the metal behaviour under the conditions of intensive electron irradiation, but they also allow one to determine the structural changes in the irradiated material.

References

[1] Dudarev E F, Kashin O A, Markov A B, Mayer A E, Tabachenko A N, Girsova N V, Bakach G P, Kitsanov S A, Zhorovkov M F, Skosyrskii A B and Pochivalova G P 2011 *Rus. Phys. J.* **54** 713–720
[2] Dudarev E F, Markov A B, Mayer A E, Bakach G P, Tabachenko A N, Kashin O A, Pochivalova G P, Skosyrskii A B, Kitsanov S A, Zhorovkov M F and Yakovlev E V 2013 *Rus. Phys. J.* **55** 1451–1457
[3] Gnyusov S F, Rotshtein V P, Mayer A E, Rostov V V, Gunin A V, Khishchenko K V and Levashov P R 2016 *Int. J. Fract.* **199** 59–70
[4] Yalovets A 1997 *J. Appl. Mech. Tech. Phys.* **38** 137–150
[5] Ashitkov S I, Komarov P S, Struleva E V, Agranat M B, and Kanel G I 2015 *JETP Lett.* **101** 276–281
[6] Ashitkov S I, Komarov P S, Struleva E V, Agranat M B, Kanel G I and Khishchenko K V 2015 *J. Phys.: Conf. Ser.* **653** 012001
[7] Mayer A E and Krasnikov V S 2011 *Eng. Fract. Mech.* **78** 1306–1316
[8] Mayer A E and Mayer P N 2015 *J. Appl. Phys.* **118** 035903
[9] Mayer P N and Mayer A E 2016 *J. Appl. Phys.* **120** 075901
[10] Kolgatin S N and Khachatur'yants A V 1982 *Teplofiz. Vys. Temp.* **20** 90–94
[11] Fortov V E, Khishchenko K V, Levashov P R and Lomonosov I V 1998 *Nucl. Instrum. Meth. Phys. Res. A.* **415** 604–608
[12] Evdokimov O B and Yalovets A P 1974 *Nucl. Sci. Eng.* **55** 67–75
[13] Plimpton S 1995 *J. Comp. Phys.* **117** 1–19
[14] Krasnikov V S, Kuksin A Yu, Mayer A E and Yanilkin A V 2010 *Phys. Solid State* **52** 1386–1396
[15] Yanilkin A V, Krasnikov V S, Kuksin A Yu and Mayer A E 2014 *Int. J. Plast.* **55** 94–107
[16] Mayer A E, Mayer P N, Krasnikov V S and Voronin D S 2015 *J. Phys.: Conf. Ser.* **653** 012093
[17] Krasnikov V S and Mayer A E 2015 *Int. J. Plast.* **74** 75–91
[18] Pogorelko V V and Mayer A E 2015 *Mater. Sci.: Eng.: A* **642** 351–359
[19] Krasnikov V S, Mayer A E and Yalovets A P 2011 *Int. J. Plast.* **27** 1294–1308
[20] Mayer A E, Khishchenko K V, Levashov P R and Mayer P N 2013 *J. Appl. Phys.* **113** 193508
[21] Mayer A E and Krasnikov V S 2015 Atomistic and continuum modeling of non-equilibrium melting of aluminum (Preprint arXiv:1512.07891v1 [cond-mat.mtrl-sci])

Acknowledgments

The development of the multiscale fracture model is supported by the Russian Science Foundation (Project No. 14-11-00538). The development of the plasticity model is supported by the Ministry of Education and Science of the Russian Federation (competitive part of State Task of NIR CSU No. 3.1334.2014/K) and by the grant from the President of the Russian Federation (Project No. MD-7481.2016.1). The investigation of the foamed melt dynamics is supported by the grant from the President of the Russian Federation (Project No. MK-9111.2016.8). The development of the non-equilibrium melting model is supported by the Russian Foundation for Basic Research (Project No. 15-32-21039).